 CMS NOTE 2000/038

The Compact Muon Solenoid Experiment

# CMS Note

Mailing address: CMS CERN, CH-1211 GENEVA 23, Switzerland

12 May 2000

# $B_s^0$ oscillation sensitivity study in CMS

Z.Xie, F.Palla, A.Starodumov

*INFN Pisa, Italy*

## Abstract

This note presents a study on the sensitivity range of $B_s^0$ mixing frequency $x_s$ and the maximum value of $x_s$ one can measure on the CMS detector. The results are obtained for the decay channel $B_s^0 \rightarrow D_s^- \pi^+$ using Geant based CMS detector simulation. The number of events expected in the decay channel $B_s^0 \rightarrow D_s^- a_1^+$ is also shown. The analysis is based on the amplitude method. With a statistics of $10^4$ pb$^{-1}$ about 4500 $B_s^0 \rightarrow D_s^- \pi^+$ events are selected giving a sensitivity on $x_s$ up to 48.

# 1 Introduction

The $B_s^0$ oscillation frequency $x_s$ is expected to be in the range between 12.9 to 26.1 in the Standard Model[1]. Such a big value of $x_s$ makes it impossible to use the time integrated measurements in the $B_s^0$ system. To observe the time dependence of the $B_s^0$ oscillation, one has to have high statistics of $B_s^0$ and to determine the $B_s^0$ decay vertex with great precision. Due to the two difficulties no existing experiment has measured $x_s$. The current world average upper limit of the $x_s$ is $x_s > 14.0$ at CL = 95%[3]. The high production rate of $b\bar{b}$ at LHC and the high precision vertex detectors in the LHC experiments make it possible to measure the $x_s$. The goal of our analysis is to study the CMS detector sensitivity to the $x_s$ parameter. Our search for $B_s^0$ oscillations is based on exclusive $B_s^0 \to D_s^- \pi^+$ decay in which a $D_s^\pm$ is fully reconstructed. Exclusive channels have the advantage of a better $B_s^0$ purity and a better proper time resolution than the inclusive semileptonic decay channels. Exclusive (completely reconstructed) decays have better proper time resolution because there is no missing particle in the decay, the $B_s^0$ momentum and mass are known with good precision.

# 2 $B_s^0$ reconstruction

One million $b\bar{b}$ events have been generated at the LHC center of mass energy $\sqrt{s} = 14$ TeV using a simulation package [4], which is based on Monte-Carlo generators PYTHIA 5.7 and JETSET 7.4 [5], developed by the CMS b-physics group.

In the simulation, the CTEQ2L[6] structure functions and SLAC (Peterson et al [7]) fragmentation function were chosen. Minimum bias events were generated with PYTHIA steering variable MSEL=1. The event generation is stopped at the string level. If the presence of $b\bar{b}$ pairs is identified in the event, the whole event is accepted and further processed.

Events which contains $B_s^0$ are selected. The $B_s^0$ is forced to decay into the channels under study. The other $B$ hadron partner is forced to decay into a muon plus anything. Only events that contains a muon in the detector acceptance are kept and the muon from the event is used for triggering and tagging purposes. The trigger probability is parametrised by the EFFMRPC function [8] based on muon $\eta$ and $p_t$. Only triggered events are saved for further analysis.

The track finding and track fitting are done using the CMSIM114 package [9]. The TDR version of the CMS tracker with the low luminosity configuration is assumed. The full description of the tracker can be found in reference [10].

## 2.1 $B_s^0 \to D_s^- \pi^+$

$B_s^0 \to D_s^- \pi^+$ is the most promising channel for the $B_s - \bar{B}_s$ oscillation study due to several reasons: relatively large branching ratio, fully reconstructed and self-tagging final state. The flavour of $B_s^0$ at the decay time is indicated by the charge of the $D_s^\pm$ meson. To trigger on and tag the flavour of the $B_s^0$ at production time, the muon from the semileptonic decay of the associated $B$ hadron is used.

In this channel, $D_s^-$ is reconstructed via two decay modes [1]:

$$D_s^- \to \phi\pi^-; \phi \to K^+K^- \tag{1}$$

and

$$D_s^- \to K^{*0}K^-; K^{*0} \to K^+\pi^- \tag{2}$$

So far no measurements of the $B_s^0 \to D_s^- \pi^+$ branching ratio exist. According to the HQET prediction, this branching ratio is $3 \times 10^{-3}$. The production fraction of $B_s^0$ is taken as $\mathcal{P}(\bar{b} \to B_s^0)$ = 10.5%. Branching ratios of decay $B_s^0 \to D_s^- \pi$ and the two decay modes of $D_s^\pm$ are shown in the Table 1.

After one year ($10^7$ s) of LHC running at a luminosity of $L = 10^{33} cm^{-2} s^{-1}$ one expects a total of $5 \times 10^{12}$ $b\bar{b}$ events. The number of events in the decay mode $D_s^- \to \phi\pi^-$ with the associated $B$ hadron decaying into a muon, before trigger acceptance and data selection cuts, is expected to be:

[1] Unless explicitly stated otherwise, charge conjugate states are always implied.

| Decay mode | Branching ratio |
|---|---|
| $B_s^0 \to D_s^- \pi^+$ | 0.003 |
| $D_s^+ \to \phi\pi^+$ | 0.036±0.009 |
| $\phi \to K^- K^+$ | 0.491± 0.008 |
| $D_s^+ \to \bar{K}^{*0} K^+$ | 0.033±0.009 |
| $K^{*0} \to K^+\pi^-$ | 0.66±0.013 |

Table 1: Branching ratios in the $B_s^0 \to D_s^+\pi^-$ decay channel.

$$
\begin{aligned}
N &= 5 \times 10^{12} \times 2\mathcal{P}(\bar{b} \to B_s^0)\mathcal{B}(b \to \mu X)\mathcal{B}(B_s^0 \to D_s^- \pi^+)\mathcal{B}(D_s^- \to \phi\pi^-)\mathcal{B}(\phi \to K^+K^-) \\
&= 7.6 \times 10^6
\end{aligned}
$$

The other decay mode used in this study of $D_s^\pm$ is $D_s^- \to K^{*0}K^-$, $K^{*0} \to K^+\pi^-$. Though this decay mode has a larger branching ratio than the $D_s^- \to \phi\pi^-$ mode, the advantage is reduced by the fact that the $K^{*0}$ has a much broader width ($\Gamma_{K^*}$ = 50.5MeV) than the $\phi$ meson ($\Gamma_\phi$ = 4.43 MeV).

In a similar way, one obtains the expected number of events in the decay channel $B_s^0 \to D_s^-\pi^+$, $D_s^- \to K^*K$ before trigger and cuts: $N = 9.4 \times 10^6$.

## 2.2 $B_s^0 \to D_s^- a_1^+$

$B_s^0$ can also be reconstructed via decay $B_s^0 \to D_s^- a_1^+$ with $a_1^+$ decaying into three pions and $D_s^\pm$ is still reconstructed via the two decay modes: $\phi\pi^\pm$ and $K^{*0}K^\pm$. Though the branching ratio of $B_s^0 \to D_s^- a_1^+$ is larger than that of $B_s^0 \to D_s^-\pi^+$, one has six particles in the final states instead of four. This induces more losses in statistics due to track reconstruction inefficiencies and softer final state particles.

Another disadvantage of this channel is that the resonance $a_1$ has a large width ($\Gamma_{a_1}$ = 250 to 600 MeV) [3], so the number of combinatorial background is expected to be much larger.

| Decay mode | Branching ratio |
|---|---|
| $B_s^0 \to D_s^- a_1^+$ | 0.006 |
| $a_1^+ \to \rho^0\pi^+$ | $\sim$ 0.5 |
| $\rho^0 \to \pi^-\pi^+$ | $\sim$ 1 |

Table 2: Branching ratios in the $B_s^0 \to D_s^- a_1^+$ decay channel.

Taking into account branching ratios listed in Table 2, the number of events expected from this channel before trigger and cuts is 6.4×$10^6$ for $D_s^+ \to \phi\pi^+$ mode and 7.8×$10^6$ for $D_s^+ \to K^{*0}K^+$ mode.

# 3 Selection criteria

## 3.1 Track reconstruction

The CMS tracker has the capability of reconstructing all tracks in the event with $p_t > 0.9$ GeV/c and $|\eta| < 2.4$. For this reason charged particles in the events are kept if they have at least $p_t^h > 1GeV$ and $|\eta^h| < 2.4$. The tracks are reconstructed using the Forward Kalman Filter algorithm. It works starting from the hits of inner most layers, namely from the Pixel hits. The average of the efficiency is around 90% for each track[10]. In our study, the total track finding and fitting efficiency for the final state of $B_s^0$ decay varies from 55% to 67% depending on the number of tracks in the final state.

## 3.2 Trigger criteria

The single muon trigger with $|\eta| <$ 2.4 and threshold $p_t^\mu > 6.5GeV$ is used as a Level 1 trigger. The rate of this trigger is around 10 KHz at the luminosity of $\mathcal{L} = 10^{33} cm^{-2}s^{-1}$.

No algorithm for the Level-2 trigger has been decided yet for CMS. However, one study has been done on the 2nd level trigger algorithm based on the inner tracker information [11]. The result of this study is used as hypothesis for the 2nd level trigger efficiency in this note.

The idea is to read out hits from the three inner most tracker layers ( which contains about 10% of the full tracker information ) and to do a fast pattern recongnition using these hits.

The result of this study shows that this kind of $D_s^- \to \phi\pi^+$ trigger has a rate of 250 Hz. The signal efficiency is 60%. The background suppression factor is about 20 for both QCD events and $B \to \mu$ events.

### 3.3 Invariant mass distributions for signal events

The precise reconstruction capabilities of CMS tracker allows to use the mass cuts in our analysis rejecting efficiently the background thanks to the reconstruction of three ($\phi$, $D_s^-$, $B_s^0$) or four ($\phi$, $D_s^-$, $a_1^+$, $B_s^0$) different resonances. Using reconstructed tracks one can obtain the invariant mass peaks corresponding to the resonances. The invariant mass distributions are shown on Fig. 1 $\div$ 3 (a $\div$ c) for different $B_s^0$ decay channels. For example, the mass resolution of $\phi$ ($\sigma_{m_\phi}$) is 2 MeV, the mass resolution of $D_s^-$ ($\sigma_{m_{D_s}}$) is 7.1 MeV and that of $B_s^0$ ($\sigma_{m_{B_s}}$) is 18.5 MeV for the channel $B_s^0 \to D_s^-\pi^+, D_s^- \to \phi\pi^-$.

### 3.4 Helicity angle cuts

When a pseudoscalar particle ($D_s$) decays into a vector particle ($\phi$), the angular distribution is given by :

$$\frac{dN}{dcos\theta} \propto |Y_1^0|^2 \propto (cos\theta^*)^2 \qquad (3)$$

where $\theta^*$ is the angle between the $\pi^-(K^-)$ coming from the $D_s^-$ decay and one of the daughters from the $\phi(K^{*0})$ decay in the $\phi(K^{*0})$ rest frame, and it is called the helicity angle. Since the combinatorial background does not have such a spin structure, its helicity angle distribution is flat. Cuts on $cos\theta^*$ are then used to suppress a significant part of the combinatorial background.

Fig. 1 $\div$ 3 (d) show the helicity angle distributions of all four channels of interest.

### 3.5 $B_s^0$ momentum cut

The average transverse momentum of the reconstructed $B_s^0$, after the cut $p_t^{hadron} > 1$ GeV/c and $p_t^\mu > 6.5$ GeV, is above 10 GeV/c while the average transverse momentum from combinatorial background events have a relatively lower average transverse momentum. The $p_t$ distribution of $B_s^0$ and its decay products in the channel $B_s^0 \to D_s^-\pi^+$ $D_s^- \to \phi\pi^-$ are shown in Fig.5. The effectiveness of the muon trigger cut at 6.5 GeV/c is not really sharp. In the present note we also required $p_t^\mu > 6.5$ GeV in the tracker. To recuperate some fraction of events one could eventually lower this cut in the tracker.

## 4 Event selection efficiency

The total efficiency of all cuts and expected number of events in each channel per year are listed in the Table 3. One can see that produced number of events per channel and per year is huge: $6 \div 10 \times 10^6$. Preliminary selections ($p_T^h$, $|\eta^h|$ and the single muon trigger) have an efficiency from $1.6 \times 10^{-3}$ to $8.2 \times 10^{-3}$.

From the remaining listed cuts, the most significant reduction of signal events comes from the secondary vertex reconstruction ($\sim$ 50% $\div$ 60 %) and sharp cut on muon $p_T^\mu > 6.5 GeV/c$. The last cut will be done at the very beginning of the Level 2 Trigger to decrease single muon trigger rate. So, final selection has an efficiency about 10% $\div$ 15%. Assuming 50% second level trigger efficiency (apart of $p_T^\mu > 6.5$ GeV/c cut) in the $B_s^0$ decay channels (6) and (7), one can expect about 4500 signal events per one LHC year at low luminosity.

## 5 Proper time reconstruction and error estimation

### 5.1 Vertexing

The decay length of the $B_s^0$ meson is approximated as the distance between the interaction point and the $B_s^0$ decay vertex. In the simulation the interaction point is fixed. The $B_s^0$ vertex are reconstructed in the following steps:

| Parameters and cuts / Channel | 1 | 2 | 3 | 4 |
|---|---|---|---|---|
| N/year($\times 10^6$) | 7.6 | 9.4 | 6.4 | 7.8 |
| $\mu$ trigger and cuts:<br>$p_T^\mu > 6.5GeV/c$;$\|\eta^\mu\| < 2.4$<br>$p_T^h > 1GeV/c$; $\|\eta^h\| < 2.4$ | 0.0082 | 0.0055 | 0.0019 | 0.0016 |
| Track finding and fitting (FKF) | 0.67 | 0.67 | 0.55 | 0.55 |
| Preliminary mass cuts and vertex quality cuts: | | | | |
| $D_s^-$ vertex fit($Prob(\chi^2, ndf) > 0.01$) | | | | |
| $B_s^0$ vertex fit($Prob(\chi^2, ndf) > 0.01$ and $cos\alpha > 0.99$) | 0.56 | 0.58 | 0.53 | 0.51 |
| $\|M_{KK} - M_\phi\| < 10MeV/c^2$ | 0.99 | | 0.99 | |
| $\|M_{K\pi} - M_{K^*}\| < 70MeV/c^2$ | | 0.96 | | 0.99 |
| $\|M_{\pi\pi\pi} - M_{a_1}\| < 300MeV/c^2$ | | | 0.98 | 0.92 |
| $\|M_{KK\pi} - M_{D_s}\| < 20MeV/c^2$ | 0.91 | | 0.93 | |
| $\|M_{KK\pi} - M_{D_s}\| < 30MeV/c^2$ | | 0.85 | | 0.84 |
| $\|M_{KK\pi\pi\pi\pi} - M_{B_s}\| < 60MeV/c^2$ | 0.94 | 0.91 | 0.94 | 0.93 |
| $\|cos\theta^*\| > 0.4$ (0.7 for $D_s^- \to K^{*0}K^-$) | 0.93 | 0.65 | 0.93 | 0.59 |
| $t > 0.4$ ps | 0.88 | 0.87 | 0.92 | 0.86 |
| $p_T^\mu > 6.5GeV/c$ | 0.46 | 0.50 | 0.54 | 0.61 |
| $p_T^{B_s} > 10GeV/c$ | 0.73 | 0.78 | 0.77 | 0.79 |
| Level-2 trigger efficiency | 0.5 | 0.5 | 0.5 | 0.5 |
| N reconstructed/year | 2750 | 1650 | 525 | 308 |

Table 3: Event selection efficiencies and the expected number of events in four decay channels. The channel number 1 refers to $B_s^0 \to D_s^-\pi^+, D_s^- \to \phi\pi^-$; 2 to $B_s^0 \to D_s^-\pi^+, D_s^- \to K^{*0}K^-$; 3 to $B_s^0 \to D_s^- a_1^+, D_s^- \to \phi\pi^-$ and 4 to $B_s^0 \to D_s^- a_1^+, D_s^- \to K^{*0}K^-$.

- Reconstruct the three particles from the $D_s^\pm$ decay.
- Combine the three tracks to form the $D_s^\pm$ vertex and form the corresponding $D_s$ "track".
- Combine the $D_s^\pm$ "track" with a single track ( the $\pi$ track or the $a_1$ "track" originating from $a_1$ vertex), which has opposite charge to the $D_s^\pm$ and reconstruct the $B_s^0$ vertex.

Fig.6 shows the residual of the $B_s^0$ decay vertex in the $x$, $y$ and $z$ directions and in space. The two Gaussian fits show that the flight path resolution in the $x$ and $y$ direction is about 30 $\mu$m and in the $z$ direction is about 50 $\mu$m. As shown in Fig.7(a)(b), the mean flight path in the transverse plane is about 1.7 mm and in space about 2.4 mm. Fig.7(c)(d) show the secondary vertex error projected along the flight path in the transverse plane and in space respectively. The error on the $B_s^0$ flight path is about 60$\mu$m in the transverse plane and 90 $\mu$m in space.

## 5.2 Proper time resolution

The proper time of the decay of a $B_s^0$ is :

$$t = \frac{l m_{B_s^0}}{p_{B_s^0}} = lg \tag{4}$$

where $l$ is the decay length and $g$ is the boost term.

The proper time error has the contribution from both the decay length and the boost term:

$$\frac{\sigma_t}{t} = \sqrt{\frac{\sigma_g^2}{g^2} + \frac{\sigma_l^2}{l^2}} \tag{5}$$

Since the momentum resolution is small with respect to the flight path resolution, we ignore the contribution from the boost term to the proper time resolution.

The proper time distribution is plotted in four regions of true proper time and fitted with two Gaussian functions (see Fig. 8). The 4 regions are : $t^{true} < 0.4ps$ , $0.4ps < t^{true} < 1.2ps$ , $1.2ps < t^{true} < 2.5ps$ and $t^{true} > 2.5ps$. The result of the fit is shown in Table 4

| Proper time region (ps) | $t^{true}$ <0.4 | 0.4< $t^{true}$ <1.2 | 1.2< $t^{true}$ <2.5 | $t^{true}$ >2.5 |
|---|---|---|---|---|
| $A_1$ | 144.4 | 143.4 | 122.5 | 89.6 |
| $\sigma_1$ (ps) | 0.055 | 0.058 | 0.073 | 0.066 |
| $A_2$ | 18.2 | 30.4 | 4.7 | 13.3 |
| $\sigma_2 (ps)$ | 0.12 | 0.12 | 0.23 | 0.14 |

Table 4: The result of the fit on the proper time.$A_1$ refers to the amplitude of the core distribution while $A_2$ refers to that of the tail one ; $\sigma_1$ refers to the $\sigma$ of the core distribution while $\sigma_2$ refers to that of the tail one.

Since there is a save cut on the proper time $t > 0.4$ ps, the proper time resolution in the region $t^{true}$ <0.4 ps can be ignored. The fit shows that the second Gaussian contributes little to the overall distribution and that the $\sigma_t$ of the first Gaussian is nearly independent of the true proper time. So the proper time resolution can be expressed as a constant, $\sigma_t$ = 0.07 ps.

# 6 Extraction of $x_s$ limits and precision

## 6.1 Unbinned amplitude method

The amplitude method[2] has been used in order to evaluate the sensitivity of the analysis.

Firstly, the events are classified as mixed or unmixed according to the sign of the lepton charge and the charge of the $D_s$. For each event a probability to observe a certain combination of $B_s^0$ flavours at the production and the decay time ($t$) is constructed. The event is labelled as "like-sign", if the $D_s$ and the muon from the other $B$ hadron decay have the same sign; in this case, the probability is $\mathcal{P}_{like}$, if the $D_s$ and the $\mu$ are of opposite sign then the probability is $\mathcal{P}_{unlike}$:

$$\mathcal{P}_{like}(t) = e^{-\frac{t}{\tau}}[\frac{1}{2}f_s(1-\eta)(1-Acos\frac{x_s t}{\tau}) + \frac{1}{2}f_s\eta(1+Acos\frac{x_s t}{\tau}) + \frac{1}{2}(1-f_s)] \tag{6}$$

$$\mathcal{P}_{unlike}(t) = e^{-\frac{t}{\tau}}[\frac{1}{2}f_s(1-\eta)(1+Acos\frac{x_s t}{\tau}) + \frac{1}{2}f_s\eta(1-Acos\frac{x_s t}{\tau}) + \frac{1}{2}(1-f_s)] \tag{7}$$

where $f_s$ is the signal purity, $\eta$ is the mistagging probability. The first term in each equation describes the probability for correctly tagged signals and the second term comes from the mistagged events. The third term describes the probability for the background events, assuming that it has an exponential behaviour, and the same proper time of the signal. In the case of pure $B_s^0$ samples ($\eta = 0$, $f_s = 1$) the $\mathcal{P}_{like}$ describes the probability that an oscillation has occurred, while $\mathcal{P}_{unlike}$ is the probability of no oscillation.

The measured proper time is affected by the experimental resolution. In order to take this into account the $\mathcal{P}_{like}$ and $\mathcal{P}_{unlike}$ functions are convoluted with a resolution function $R(t-t')$:

$$\tilde{\mathcal{P}}(t) = \mathcal{P}(t') \otimes R(t-t'). \tag{8}$$

As it has been shown in paragraph 5.2, for CMS $R(t-t')$ is well described by a single Gaussian of $\sigma_t$ = 0.07 ps.

$$R(t-t') = \frac{1}{\sqrt{2\pi}\sigma_t} e^{-\frac{(t-t')^2}{2\sigma_t^2}} \tag{9}$$

A fit to the reconstructed proper time distribution of the events tagged as mixed and unmixed is performed for each fixed value of the oscillation frequency $x_s$, while its amplitude $A$ is left as a free parameter. This is done by minimising the likelihood $\mathcal{L}$:

$$\mathcal{L} = \prod_{i=1}^{N_{like}} \tilde{\mathcal{P}}_{like}(t) \prod_{i=1}^{N_{unlike}} \tilde{\mathcal{P}}^{unlike}(t) \tag{10}$$

A scan in the $x_s$ is performed and the amplitude is extracted at each value. The expected value of the amplitude $A$ is one if $x_s = x_s^{true}$. The range of $x_s$ for which $A$ is found to be compatible with zero and incompatible with one is excluded.

The sensitivity in $x_s$ of an analysis is the range of $x_s$ values for which the error on $A$ ($\sigma_A$) is small enough with respect to $A = 1$, so that the two values $A = 0$ and $A = 1$ can be distinguished.

The usual definition for the sensitivity is the value for $x_s$ for which a measured value $A = 0$ implies that $A = 1$ is excluded at 95 % CL. This happens when $1.645\sigma_A = 1$.

## 6.2 Fast Monte Carlo

In order to study the sensitivity of the method and to check the calibration of the amplitude curves, a fast Monte Carlo has been developed. In this analysis several parameters are used as input to simulate the proper time distribution of real experiment data. The parameters of the generation have been fixed as follows:

- The mistagging rate $\eta$ has been set to 0.22 [12]
- The signal purity $f_s$ of the sample is assumed to be equal to 0.5
- The proper time resolution has been set to a constant $\sigma_t = 0.07ps$
- $\tau_{B_s^0}$ = 1.61 ps[13].
- The number of signal events is 4500. This is the expected number of signal events in the decay channel $B_s^0 \to D_s^- \pi^+$, with $D_s^-$ decays into $\phi\pi^-$ or $K^{*0}K^-$ after one year running of LHC at low luminosity.

First, 9000 events (4500 signal and 4500 background events) are generated according to the probability function function (6) and (7). The proper time are convoluted with a Gaussian function with $\sigma_t$ = 0.07 ps. The oscillation frequency $\Delta m_s$ is scanned. For each value of $\Delta m_s$ the total likelihood function is minimised with respect to the free parameter $A$. If $\Delta m_s = \Delta m_s^{true}$, the amplitude $A$ is equal to 1 while for all other values $A$ should be distributed around $0$.

To check this, 500 Monte Carlo experiments have been simulated at each value of $\Delta m_s$. Fig. 9 shows the amplitude value averaged over 500 experiments as a function of $x_s$. The error bar indicates the error on the amplitude of each experiment averaged over 500 experiments. The average amplitude over these experiments is consistent with 1 for $\Delta m_s = \Delta m_s^{true}$ and with $0$ otherwise.

The estimate of the statistical uncertainty on the amplitude has also been verified by studying the "pull" distribution defined as $\frac{\mathcal{A}-\mathcal{A}_{true}}{\sigma_{\mathcal{A}}}$. As shown in Fig. 10, the "pull" has a mean value of $0$ and a sigma of $1$. This means that the amplitude method is not biased.

Fig. 11 shows the amplitude $\mathcal{A}$ together with its error $\sigma_{\mathcal{A}}$ as a function of $x_s$ and the dotted curve is the 1.645$\sigma_{\mathcal{A}}$ curve. This plot is the output of one experiment with the input of $x_s^{true}$ = 30. Other input parameters are those listed at the begining of this subsection and $f_s$ = 0.5. The peak in the amplitude compatible with one at $x_s$ = 30 indicates that this experiment is successful. The fact that the error $\sigma_{\mathcal{A}}$ has an exponential behaviour $\approx$ exp($\Delta m_s \sigma_t$) is due to the proper time resolution. The point where 1.645$\sigma_{\mathcal{A}}$ curve meets 1 indicates the sensitivity of this experiment.

## 6.3 $x_s$ sensitivity and limits

In a real measurement, one cannot measure the $x_s$ value up to $x_s^{sens}$ due to the fluctuations and also to the systematic uncertainties. While the sensitivity $x_s^{sens}$ indicates the maximum value that a certain experiment can exclude, we define a 95%CL limit ($x_s^{95CL}$) to indicate the maximum $x_s$ that one experiment can measure with 95% probability.

The $x_s^{95CL}$ is extracted by making 1000 'experiments' for each $x_s$ value. Each experiment has the same condition (mistagging, signal purity, proper time resolution, etc) but independent samples.

The 95% CL limit of the experiment is the maximum $x_s$ one can reach for which 95% of the 1000 'experiments' are successful. An experiment is called 'successful' when a $x_s$ corresponds to the highest peak in the amplitude spectrum and it is by the vicinity of the $x_s^{true}$, say within the natural width ($\pm 1.5$ in $x_s$) of the amplitude distribution, which can be seen in Fig. 9. [2)]

Fig.12 shows the sensitivity and 95%CL limit of $x_s$ as a function of the integrated luminosity. One can see that the two lines are not exactly parallel. The 95% CL curve is going to fall down means that with too small number of events one cannot measure $x_s$ at all. However, one can always exclude certain $x_s$ values.

Fig.13 shows the 95%CL limit of $x_s$ as a function of the signal purity $f_s$. From the plot one can see that having 4500 signal events is sufficient to the signal to background ratio variation as there is some kind of plateau as a function of signal to background ratio. The signal purity $f_s$ increases from 0.2 to 1 (number of background decreases from 18,000 events), the variation in 95% limit is only about 10%.

# 7 Conclusion

After one year of LHC running at the low luminosity, about 4500 events are expected to be collected in the $B_s^0$ decay channel $B_s^0 \to D_s^- \pi^+$ with $D_s^-$ further decaying into $\phi\pi^-$ or $K^{*0}K^-$. The GEANT based simulation with detailed tracker system description shows that the proper time resolution of this decay channel in CMS is 0.07 ps. With this statistics and the proper time resolution, assuming the signal to background ratio 1:1, the region $x_s < 48$ can be excluded with 95% CL. Under the same condition, one expects to measure $x_s$ up to 43. When varying the signal/background to 1:4 the limit changes to 40. After three years of LHC running under the low luminosity, the region $x_s < 55$ can be excluded and one expects to measure $x_s$ up to $x_s = 50$.

[2)] This criteria is chosen to be compatible with reference [14].

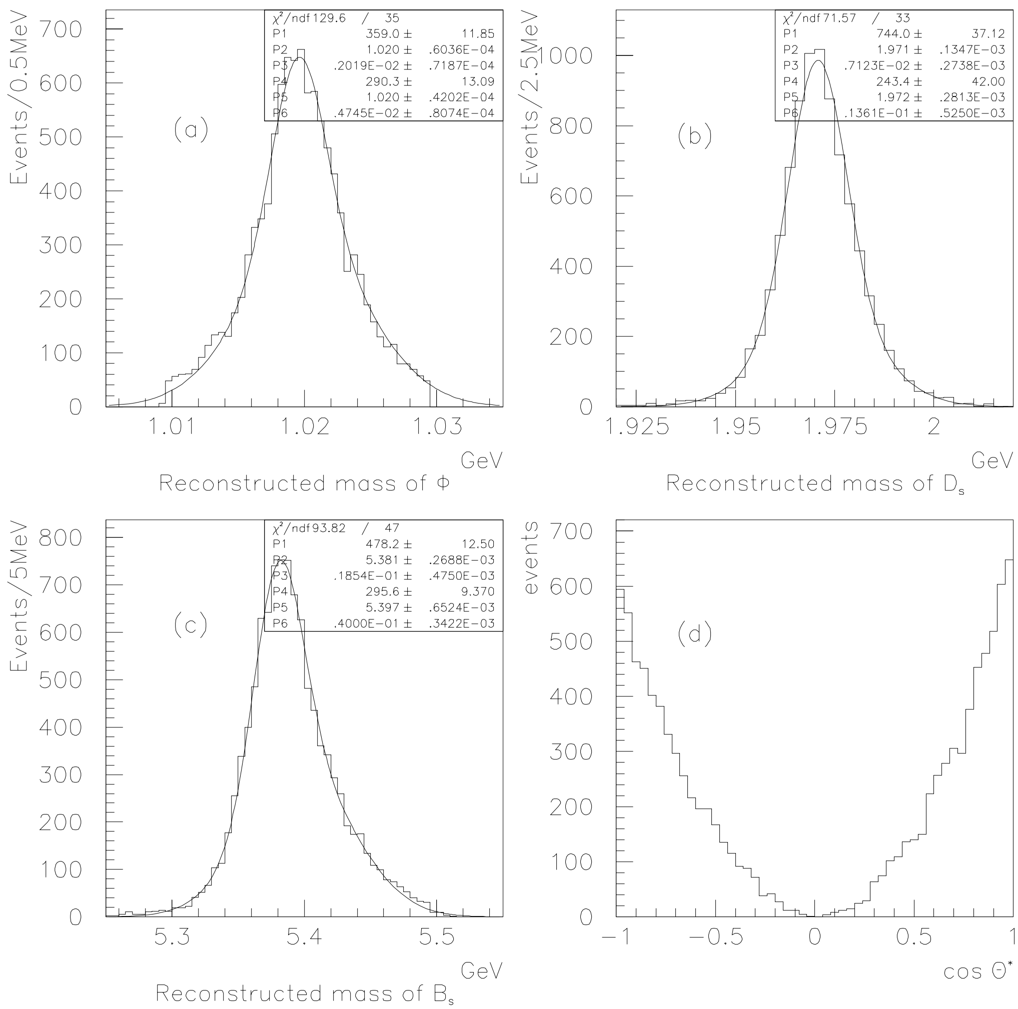


Figure 1: Reconstructed mass and helicity angle distribution of channel $B_s^0 \to D_s^- \pi^+; D_s^- \to \phi\pi^-$.

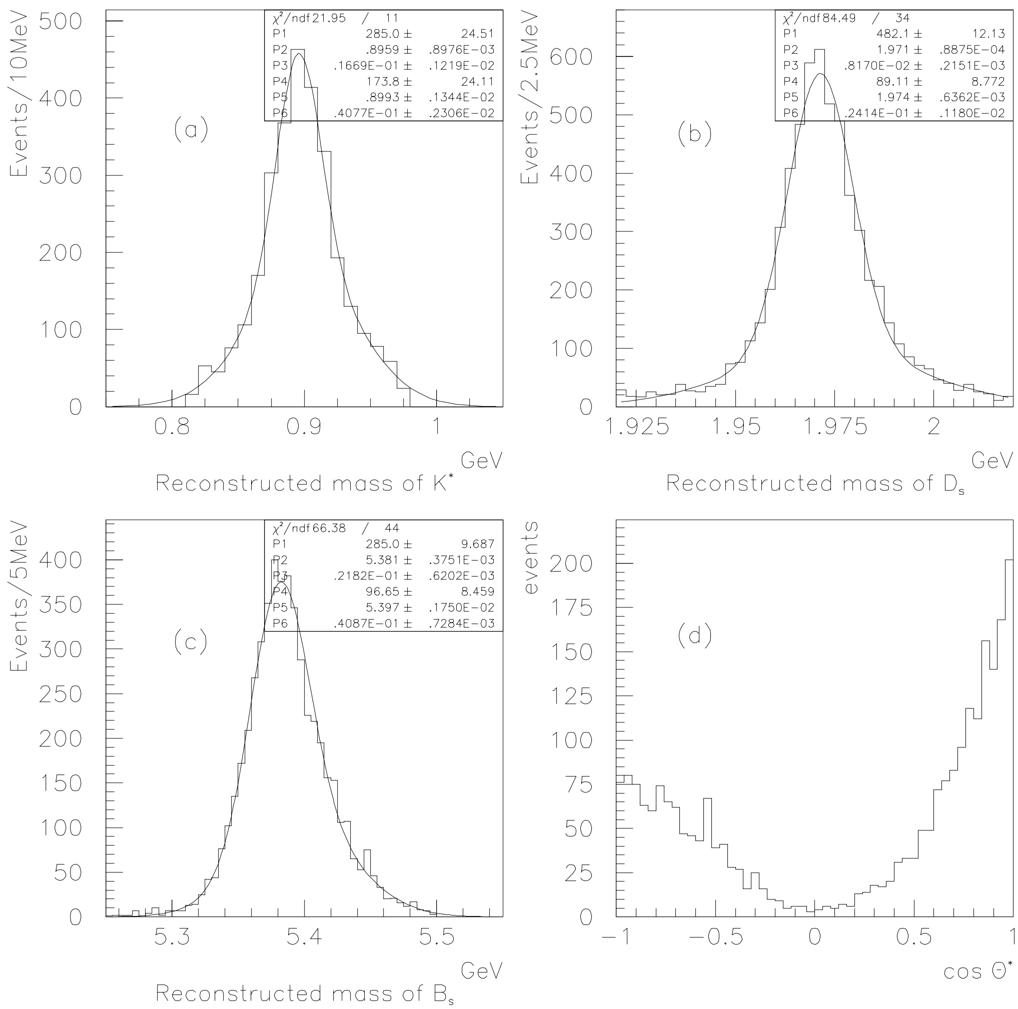


Figure 2: Reconstructed mass and helicity angle distribution of channel $B_s^0 \to D_s^- \pi^+; D_s^- \to K^{*0} K$.

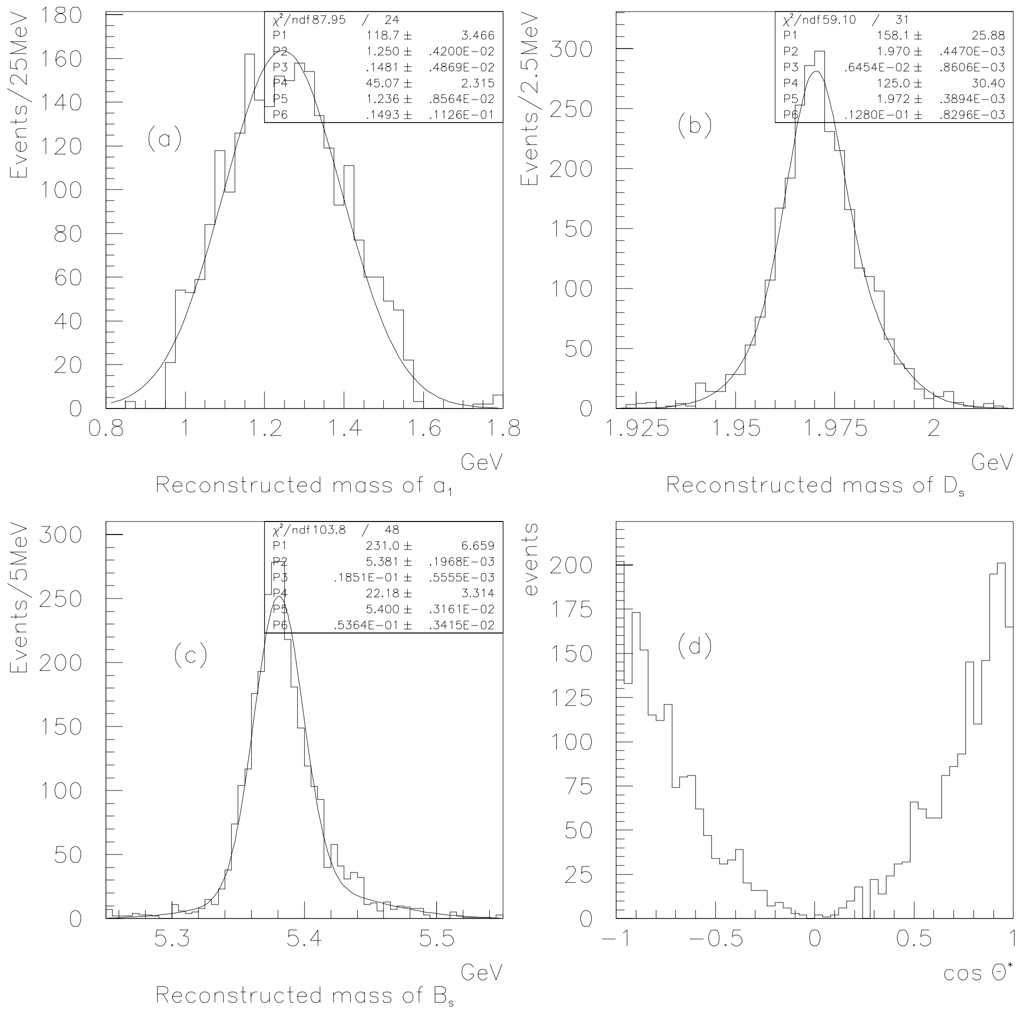


Figure 3: Reconstructed mass and helicity angle distributions of channel $B_s^0 \to D_s^- a_1^+; D_s^- \to \phi\pi^-$.

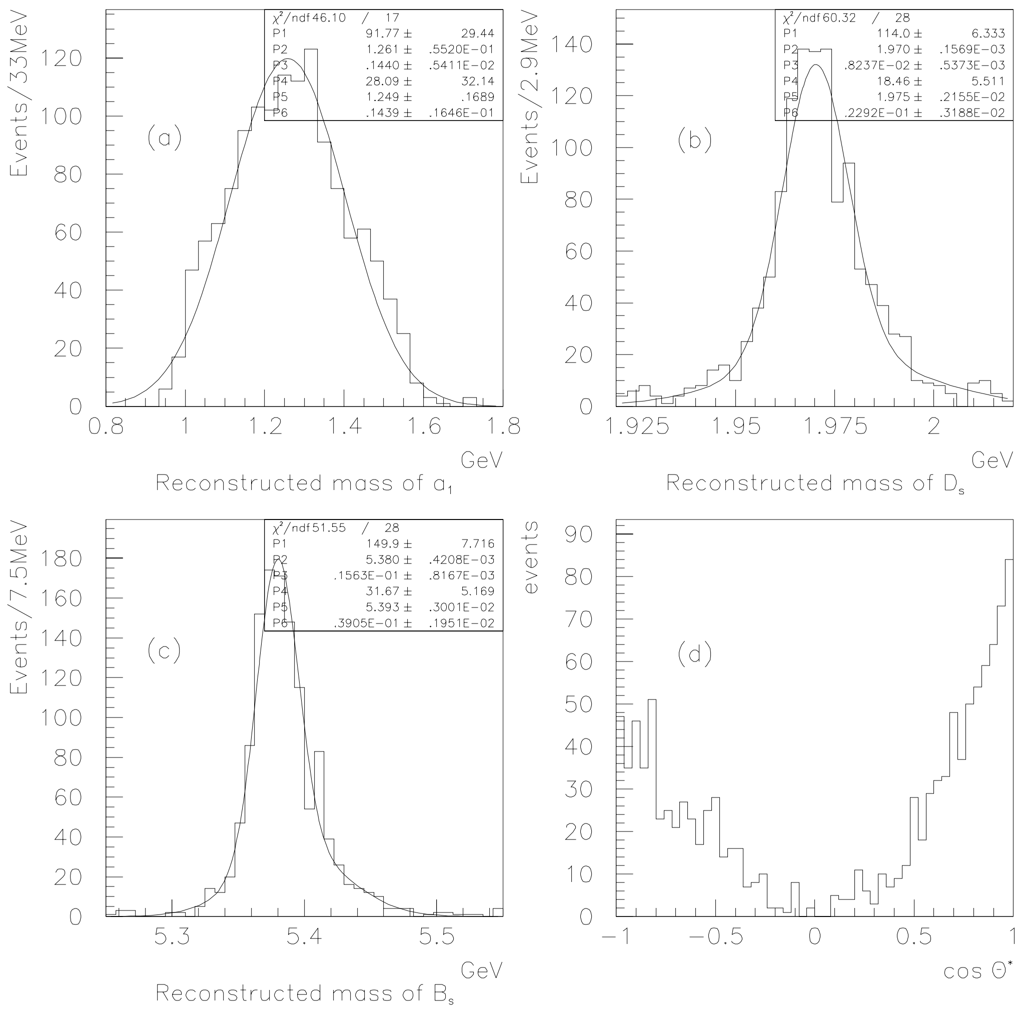


Figure 4: Reconstructed mass and helicity angle distributions of channel $B_s^0 \to D_s^- a_1^+; D_s^- \to K^* K$.

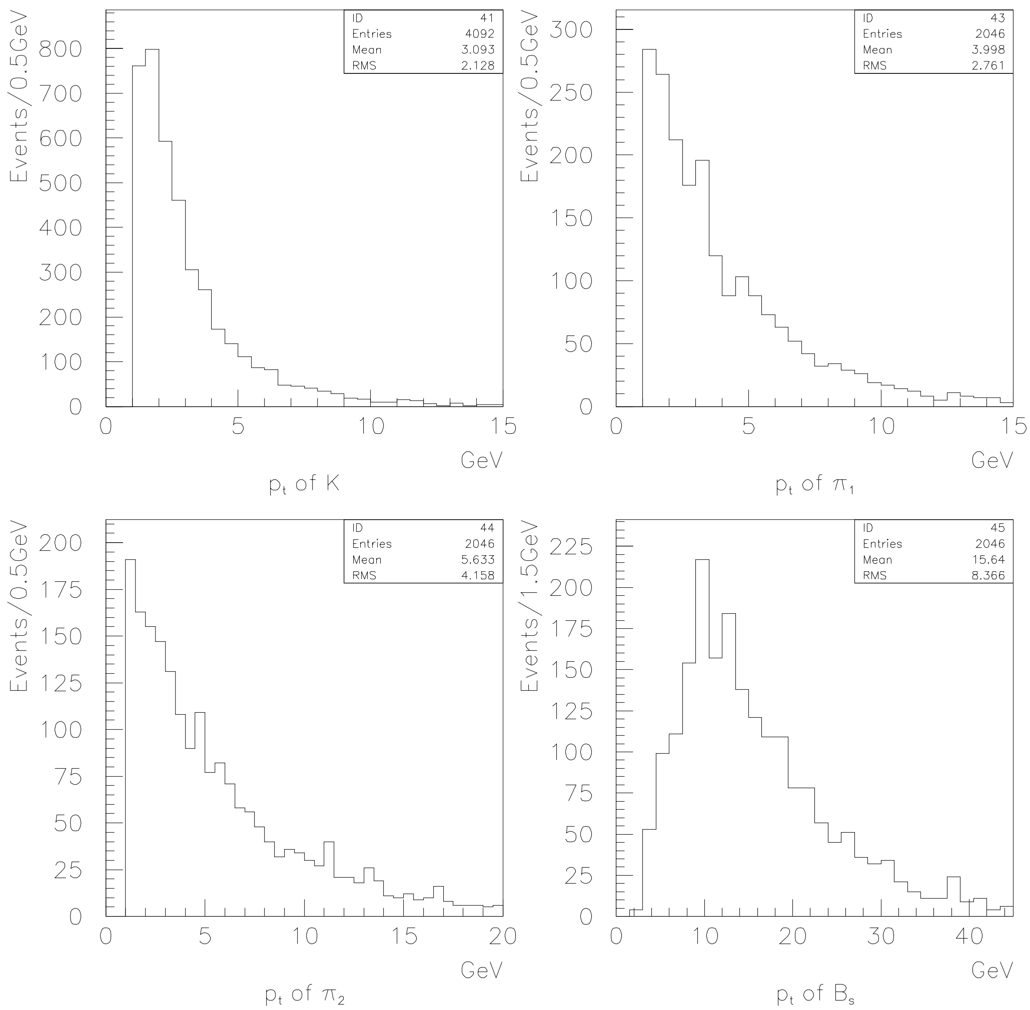


Figure 5: $p_t$ distributions of tracks and $B_s^0$ in the channel $B_s^0 \to D_s^- \pi^+; D_s^- \to \phi\pi^-$.

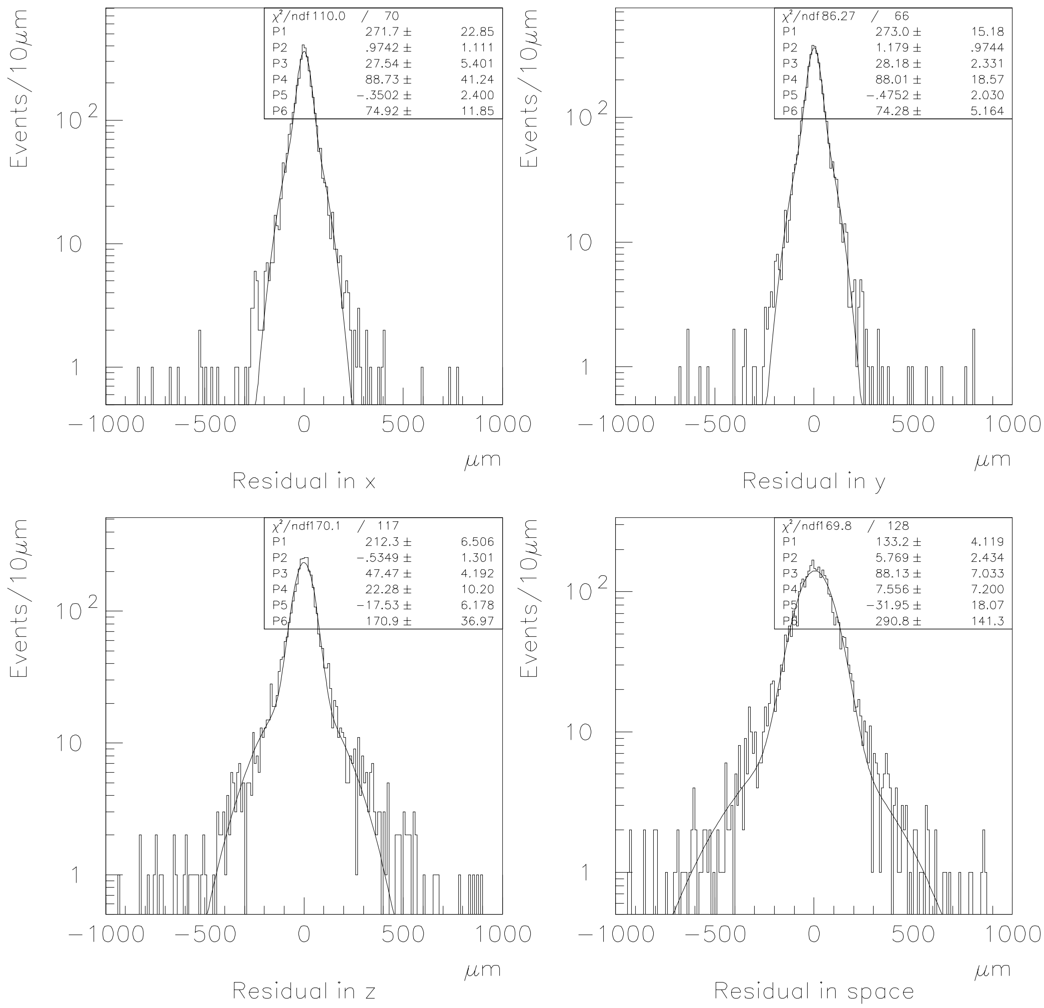


Figure 6: Residuals of the $B_s^0$ decay vertex in the $x$, $y$ and $z$ directions and in space

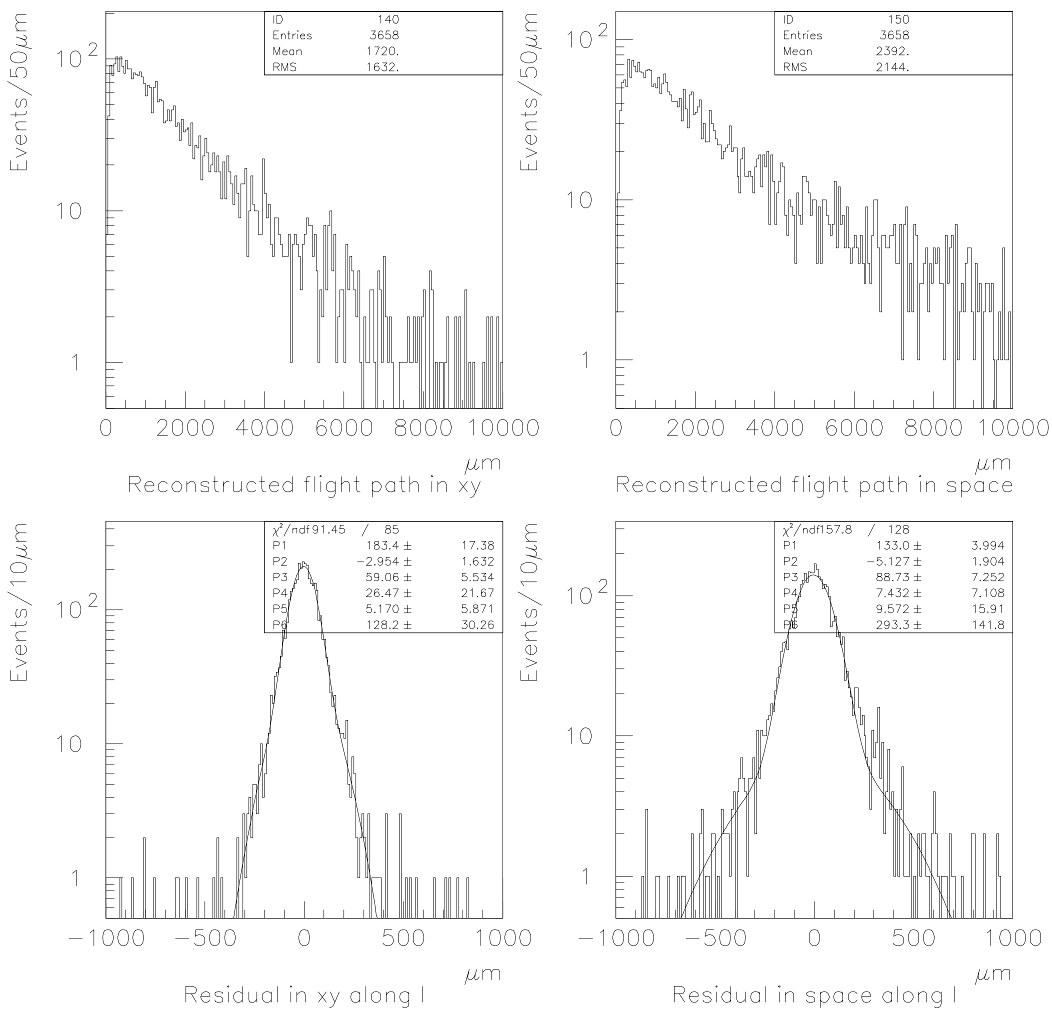


Figure 7: (a) Reconstructed $B_s^0$ flight path in the transverse plane. (b) Reconstructed $B_s^0$ flight path in space. (c)$B_s^0$ decay vertex error projected along $B_s^0$ flight path direction in the transverse plane.(d)$B_s^0$ decay vertex error projected along $B_s^0$ flight path direction in space.

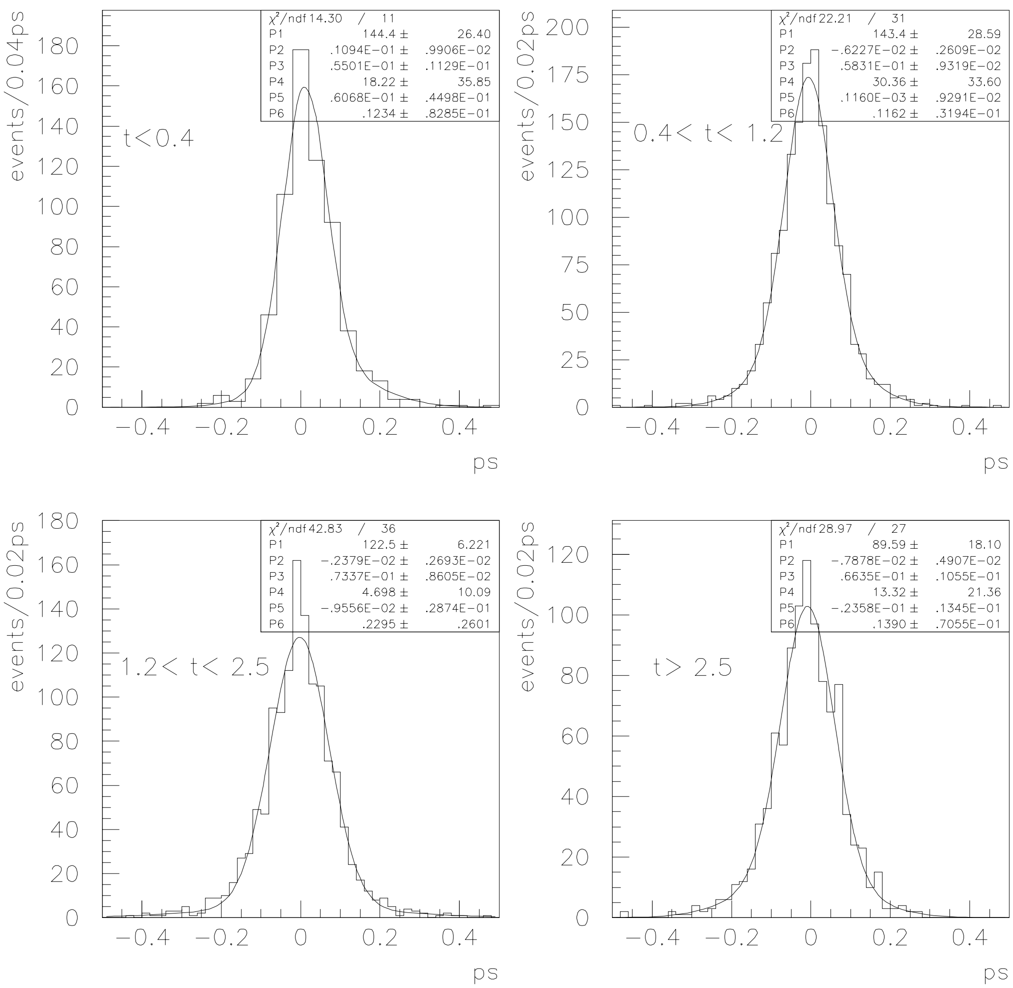


Figure 8: The proper time resolution in various intervals of true proper time $t^{true}$ (in ps).

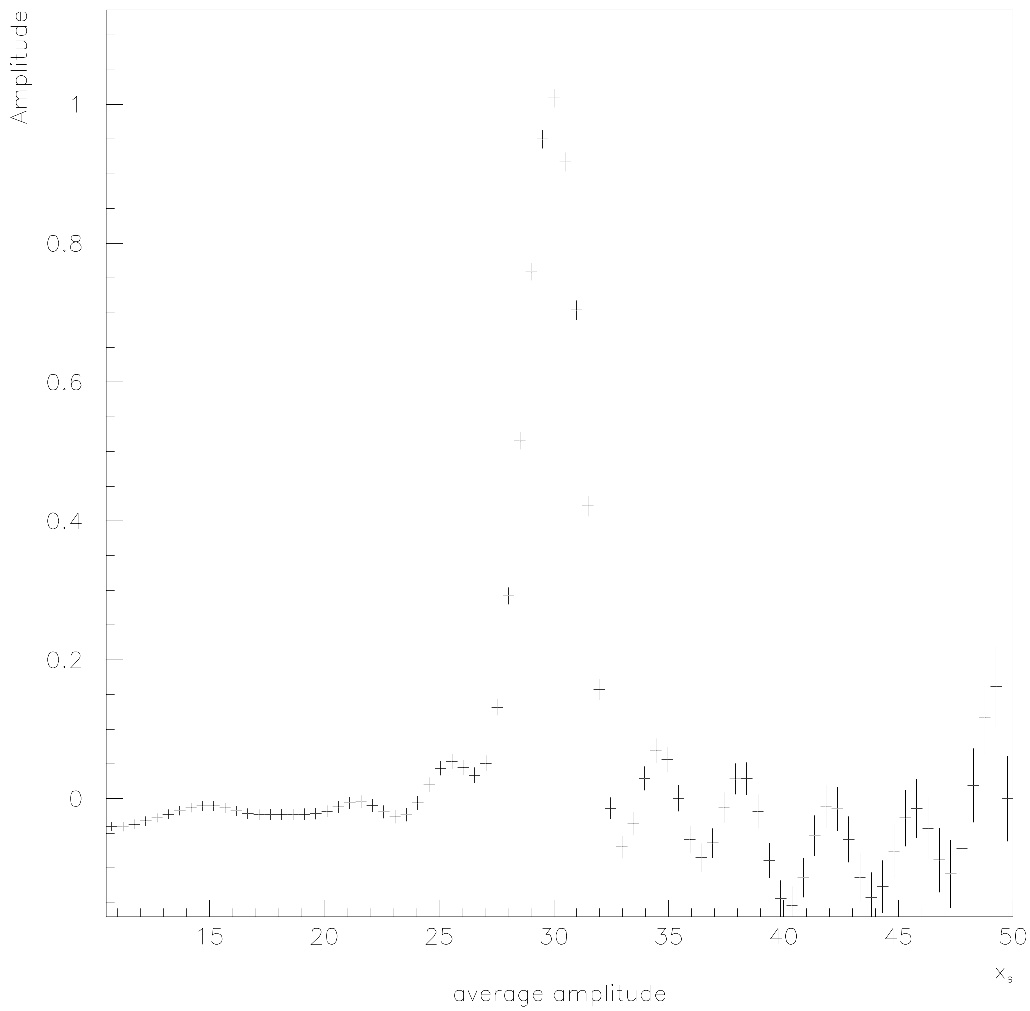


Figure 9: Average amplitude of 500 experiments.

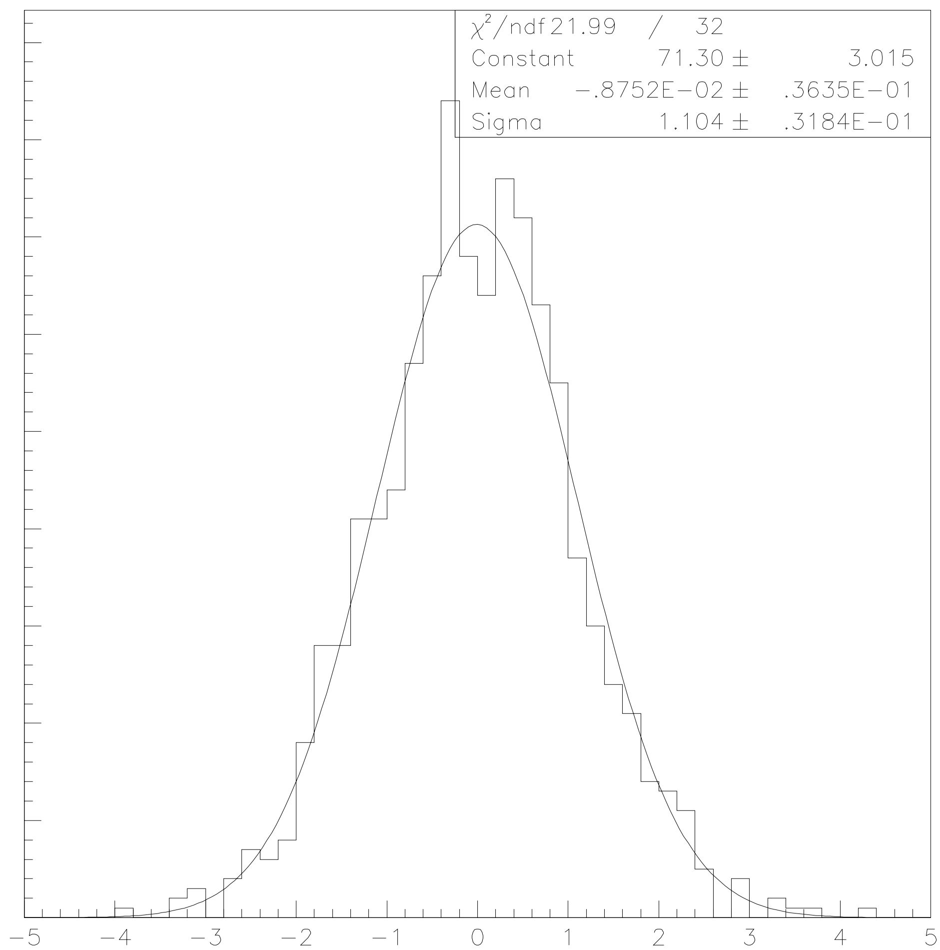


Figure 10: Pull distribution of amplitude $A$.

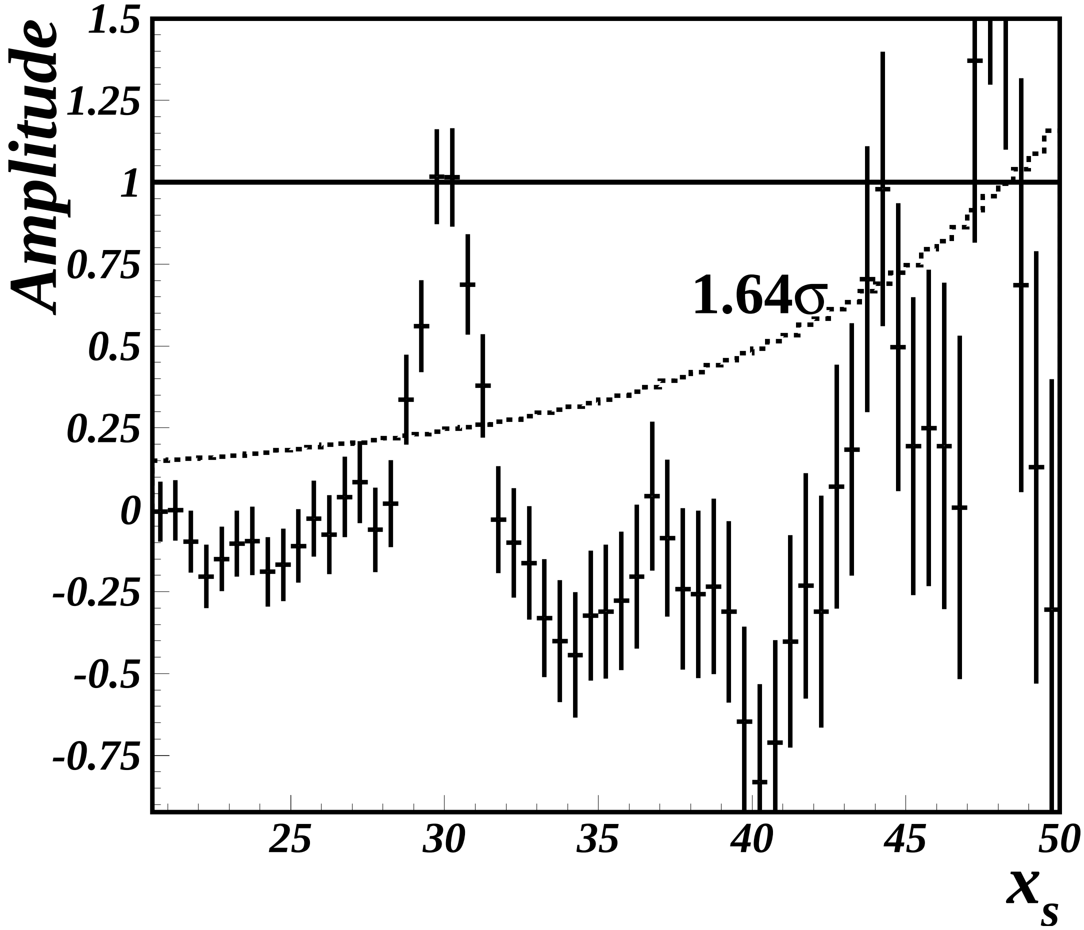


Figure 11: Amplitude $\mathcal{A}$ (histogram) and 1.645 $\sigma_{\mathcal{A}}$ (dashed line) distribution for $x_s^{true}$=30. The error bar in $y$ refers to the corresponding $\sigma_{\mathcal{A}}$.

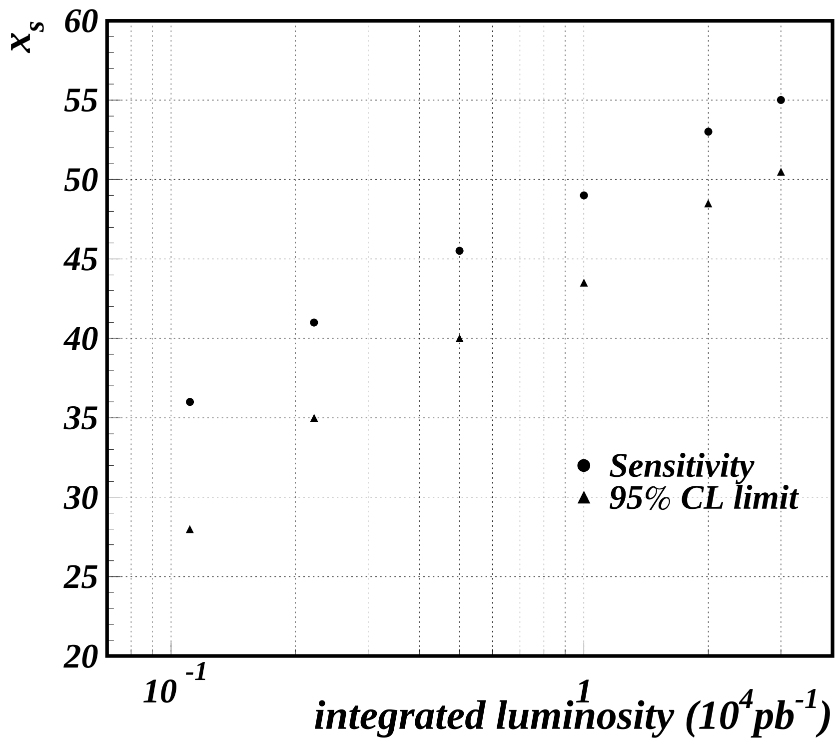


Figure 12: The sensitivity and the 95% CL limit of $x_s$ as a function of the integrated luminosity.

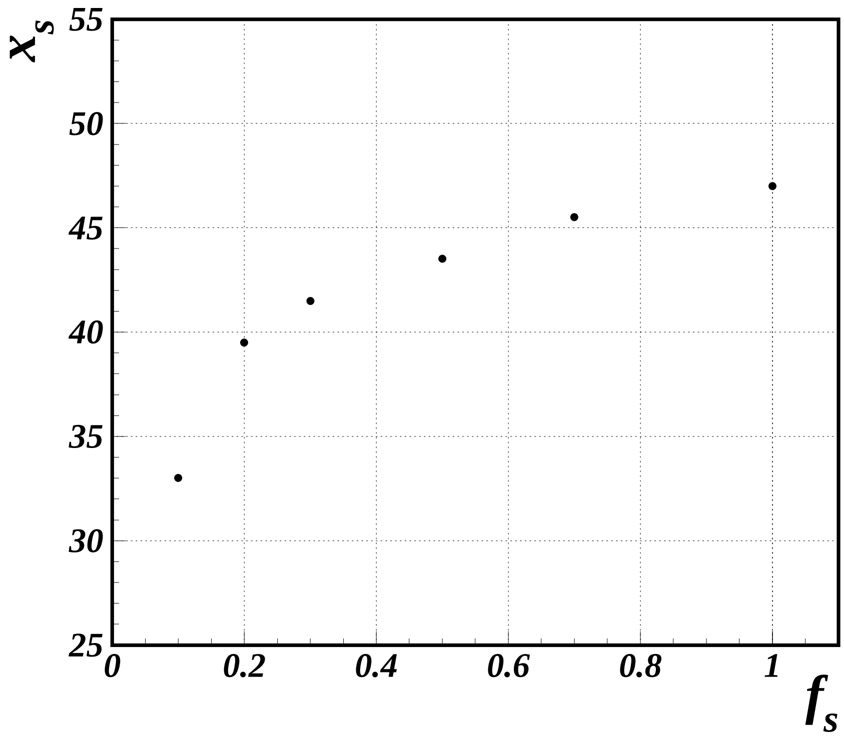


Figure 13: The 95% CL limit of $x_s$ as a function of the signal purity $f_s$.

# References

[1] A.Ali and D.London, **Nuclear Physics B(Proc.Suppl.) 54A(1997) 297.**

[2] H.-G. Moser and A.Roussarie, **PUB 96-005 CERN/PPE**

[3] Particle Data Group, **Review of Particle Physics (1998)**.

[4] M. Konecki, A.Starodumov, $b\bar{b}$ **Events simulation package user's manual**.

[5] T. Sj$\ddot{o}$strand, **Comput. Phys. Commun. 82 (1994) 74**

[6] J.Botts et al., **Phys. Lett. B304 159 (1993).**

[7] C.Peterson et al., **Phys. Rev. D 27 (1983) 105.**

[8] M.Konecki et al., **CMS TN/96-104 (1996).**

[9] CMS detector simulation softeware group, **CMSIM User's Guide (1998).**

[10] CMS Tracker Tecnical Design Report, **CERN/LHCC 98-6.**

[11] A.Starodumov at TriDAS week Nov. 1998, **http://cmsdoc.cern.ch/distribution/tridas/Mettings/TriDAS weeks/98.11.09/HLT-AS.pdf**

[12] M. Konecki, **CMS-TN/96-105.**

[13] Particle Data Group, **Physical Review D (1996).**

[14] S. Gadomski et al., **hep-ex/9611001 (1996).**